



Polymeric micelles for pH-responsive lutein delivery

Dongxue Zhang^a, Lina Wang^b, Xin Zhang^b, Decai Bao^{a,*,**}, Yanjun Zhao^{b,*}

^a College of Chemistry and Chemical Engineering, Bohai University, Jinzhou, 121013, China

^b School of Pharmaceutical Science & Technology, Tianjin Key Laboratory for Modern Drug Delivery & High Efficiency, Collaborative Innovation Center of Chemical Science and Engineering (Tianjin), Tianjin University, 92 Weijin Road, Nankai District, Tianjin, 300072, China



ARTICLE INFO

Keywords:

Micelles
Drug delivery
Lutein
pH-responsive
Controlled release

ABSTRACT

There has been growing interests in nanoparticulate delivery of the natural carotenoid, lutein for anti-cancer therapy. However, the low aqueous solubility of lutein and the poor lutein release from nanocarriers limit its bioavailability and therapeutic outcome. To address this problem, we report a pH-responsive polymer micelle for on-demand delivery of lutein. The selected micelle building polymer was methoxy poly(ethylene glycol)-*co*-poly(aspartic acid)-imidazole that was ionically crosslinked by biocompatible iron (III). Such imidazole-iron coordination bonding is stable in neutral conditions (e.g. pH 7.4), but it could be ruined under acidic micro-environment (e.g. endosome). A control micelle was also produced with non-responsive PEGylated poly(β -benzyl *L*-aspartate) (mPEG-PBLA) copolymer. The drug-loaded responsive micelles displayed a hydrodynamic size of 168.2 nm with a lutein loading of 3.5% (w/w) and iron loading of 0.2% (w/w). The pH-responsive release was verified by *in vitro* release test at pH 7.4 and 5.0. The half maximal inhibitory concentration of the responsive micelles in HeLa cells was ca. 58.4 μ M that was significantly lower than that of control micelles. All the results suggested that the triggered cargo release aided the cytosol accumulation of lutein without the delay of therapeutic action. The current work highlighted the stimuli-responsive nanomedicine in on-demand carotenoid delivery.

1. Introduction

Lutein, as a natural carotenoid, is widely found in bananas, kiwifruit and marigold plants and plays an important role in maintaining human health [1]. As an antioxidant, the effect of lutein in prevention and treatment of various eye diseases has been demonstrated [2]. Besides these, lutein also displays a preventive and inhibitory effect for many diseases, such as cancer [3]. Lutein has also been found able to reduce cisplatin-induced renal damage [4]. However, lutein is very unstable in nature because it is an isoprenoid compound with multiple conjugated double bonds, which makes it very easily isomerized, oxidized and degraded [1]. Meanwhile, lutein is highly hydrophobic which severely affects its absorption and bioavailability in the body [5]. With the rapid development of nanobiotechnology, there has been growing application of nanocarriers for lutein solubilization and stabilization for enhanced bioavailability and therapeutic outcomes [6–10].

Nanoparticulate drug delivery has to balance the premature dose dumping and rapid on-demand drug release in target sites [11–13]. The typical strategy is to select a carrier with a high affinity with the cargo to ensure a high drug loading and good stability of nanocarrier during

systemic circulation [14]. However, this can result in the poor drug release upon particle reaching the target location [12]. The employment of stimuli-responsive nanocarriers has been a popular approach to address this issue [15]. A diverse range of internal and external triggers can be utilized to design responsive nanomedicines, including pH, redox potential, reactive oxygen species, heat, magnetic field, light, and ultrasound [16–20]. Among these, the pH trigger is unique as the blood circulation maintained a neutral condition, whereas the intracellular endosome is acidic. Upon endocytosis, the low pH microenvironment in the endosome/lysosome provides an excellent trigger to initiate drug release [21,22].

Our recent work reported an imidazole-bearing polymer micelle that displayed both singlet oxygen- and pH-sensitive cargo release behavior; the polymer was methoxy poly(ethylene glycol)-*co*-poly(aspartic acid)-imidazole (mPEG-PAsp-IM) [19]. The pH-sensitivity of such micelles lies in the distinct pKa of imidazole moiety (ca. 6–7) [23]. The imidazole moiety can also coordinate with various types of ions e.g. zinc and iron [19,24]. The coordination bonds are stable under neutral pH, but the ionization of imidazole would breakdown the bonds at the elevated proton conditions (i.e. in the endosome/lysosome) to aid drug

* Corresponding author. College of Chemistry and Chemical Engineering, Bohai University, 19 Keji Road, Songshan District, Jinzhou, 121013, China.

** Corresponding author. School of Pharmaceutical Science & Technology, Tianjin Key Laboratory for Modern Drug Delivery & High Efficiency, Collaborative Innovation Center of Chemical Science and Engineering (Tianjin), Tianjin University, 92 Weijin Road, Nankai District, Tianjin, 300072, China.

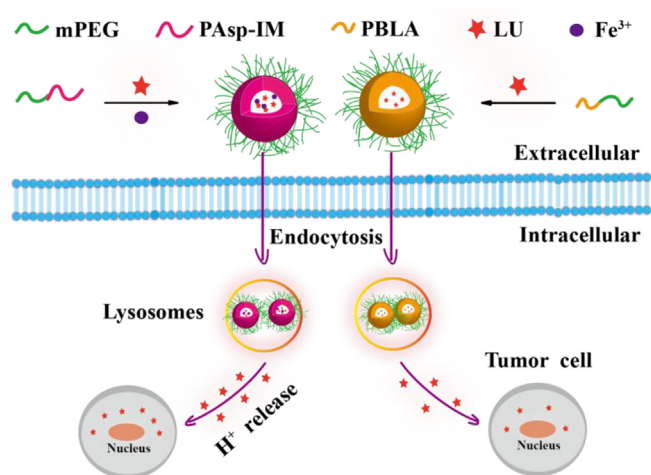
E-mail addresses: baodecai@bhu.edu.cn (D. Bao), zhaoyj@tju.edu.cn (Y. Zhao).

<https://doi.org/10.1016/j.jddst.2018.03.023>

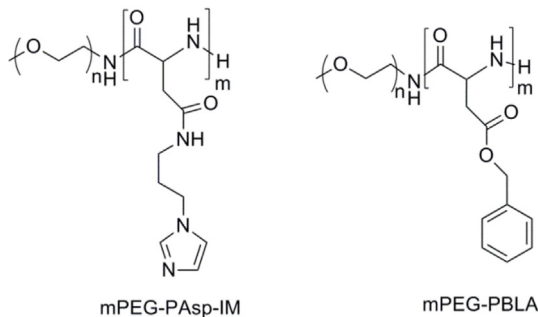
Received 30 January 2018; Received in revised form 8 March 2018; Accepted 18 March 2018

Available online 19 March 2018

1773-2247/ © 2018 Elsevier B.V. All rights reserved.



Scheme 1. Illustration of pH-responsive micelles for triggered lutein (LU) delivery. The responsive micelles (RM) and control micelles (CM) were made of methoxy poly(ethylene glycol)-*co*-poly(aspartic acid)-imidazole (mPEG-PAsp-IM) copolymers, methoxy poly(ethylene glycol)-*co*-poly(β -benzyl *L*-aspartate) (mPEG-PBLA) copolymers, respectively. Iron (III) was used to crosslink the RM for enhanced nanocarrier stability.



Scheme 2. The chemical structure of mPEG-PAsp-IM and mPEG-PBLA.

release [25,26]. Hence, the coordination-crosslinked imidazole-bearing polymeric micelles could be an ideal platform for triggered on-demand drug release. The aim of this study was to control the release of lutein in HeLa cells *in vitro* using imidazole-bearing mPEG-PAsp-IM micelles that respond to endosomal pH (Scheme 1). The non-responsive micelles made of methoxy poly(ethylene glycol)-*co*-poly(β -benzyl *L*-aspartate) (mPEG-PBLA) were used as control (Scheme 2). The anti-cancer efficacy was assessed in human cervical cancer cells (HeLa cells).

2. Experimental section

2.1. Materials

Lutein (90% food grade) was purchased from Titan Scientific Co., Ltd. (Shanghai, China). Dimethyl sulfoxide-*d*₆ (DMSO-*d*₆) and chloroform-*d* were obtained from Jinouxiang Science & Technology Co., Ltd. (Beijing, China). *L*-Aspartic acid β -benzyl ester was purchased from Beijing HWRK Chem Co., Ltd. (Beijing, China). Triphosgene (BTC) and 1-(3-Aminopropyl) imidazole (IM) were sourced from Sigma-Aldrich (Beijing, China). Methoxypolyethylene glycol amino (mPEG-NH₂, 5000 Da) was purchased from Shanghai Ponsure Biotech, Inc. (shanghai, China). Sodium hydroxide and 3-morpholinopropane-sulfonic acid (MOPS), nitrilotriacetic acid, ferric chloride (FeCl₃), sodium dihydrogen phosphate (NaH₂PO₃), citric acid, sodium dodecyl sulfonate (SDS) were obtained from Guangfu Fine Chemical Research Institute (Tianjin, China). Tetrahydrofuran (THF), hexane, *N,N*-dimethylformamide (DMF), trichloromethane (CHCl₃), diethyl ether, dimethyl sulfoxide, concentrated hydrochloric acid (HCl) were purchased

from Jiangtian Chemicals (Tianjin, China). Acetonitrile (ACN) and methanol were purchased from Tianjin Concord Technology Co., Ltd. (Tianjin, China). 3-[4, 5 dimethylthiazol-2-yl]-2, 5 diphenyltetrazolium bromide (MTT), Annexin V-FITC/PI Apoptosis Detection Kit was purchased from Yeasen Biotechnology Co., Ltd. (Shanghai, China). Triton X-100, propidium iodide (PI) and RNase were purchased from Solarbio Science Technology Co., Ltd. (Beijing, China).

2.2. Synthesis of mPEG-PBLA and mPEG-PAsp-IM

The synthesis of mPEG-PBLA was based on a previously published method [19]. The β -benzyl *L*-aspartate *N*-carboxyanhydride (BLA-NCA) was first synthesized. Briefly, BLA (2.5 g, 11.2 mmol) and BTC (1.7 g, 5.7 mmol) were dissolved in 15 mL anhydrous THF under nitrogen protection. The solvent was stirred at 50 °C for 3 h. The mixture was then concentrated to 5 mL and added to 20 mL ice-cold hexane. The precipitates were purified by recrystallization in THF and *n*-hexane (yield: 89%). The mPEG-PBLA was synthesized with the mPEG-NH₂ as the initiator to induce the polymerization of BLA-NCA. In brief, mPEG-NH₂ (0.1 g, 0.02 mmol) was dissolved in 3 mL anhydrous CHCl₃. BLA-NCA (0.15 g, 0.6 mmol) was dissolved in 0.8 mL anhydrous DMF with nitrogen protection. Thereafter, the mixture of mPEG-NH₂ was added to BLA-NCA solution under nitrogen atmosphere. The mixture was stirred at 35 °C for 24 h and added to 100 mL iced diethyl ether. The precipitate was dissolved in DMF, followed by dialysis against water (MWCO: 3500 Da) for 24 h. The mPEG-PBLA copolymers were obtained after freeze-dried (yield: 82%). mPEG-PAsp-IM was obtained by mixing mPEG-PBLA (0.5 g, 0.05 mmol) and IM (3.58 mL, 30 mmol) in 3 mL DMSO under nitrogen atmosphere. The reaction was carried out at 40 °C for 48 h. After that, the mixture was added into 20 mL iced HCl (0.1 M) and dialyzed against HCl solution (0.01 M) (MWCO: 1000 Da) for 24 h. The mPEG-PAsp-IM copolymers were obtained after lyophilization (yield: 76%).

2.3. Micelle preparation and characterization

The preparation of responsive polymeric micelles employed a dialysis method. Briefly, mPEG-PAsp-IM or mPEG-PBLA (0.1 g, 0.01 mmol) and LU (10 mg, 0.07 mmol) were dissolved in 3 mL methanol and the solution was dialyzed against MOPS buffer (pH 7.4, 25 mM) containing Fe³⁺ (0.4 mM) and nitrilotriacetic acid (1.2 mM). A regenerated dialysis tube (MWCO: 1000 Da) was used to separate the polymer solution and the medium. After 24 h, the responsive micelles (RM) or control micelles (CM) were formed, followed by precipitate (i.e. LU) removal by centrifugation 3000 g. The solution was further dialyzed against nitrilotriacetic acid-containing MOPS buffer (pH 7.4) to remove free Fe³⁺. After 24 h, the RM or CM was obtained after lyophilization. LU recovery was calculated based on the sum from the micelles, precipitate, and dialysis medium in reference to the LU feed. The hydrodynamic diameters of micelles were determined at 25 °C by a Zetasizer Nano ZS (Malvern Instrument Ltd., Malvern, UK). The iron content of the samples was measured via 180-80 polarized Zeeman atomic absorption spectrophotometer (Hitachi High-Technologies Co. Ltd., Shanghai, China). The drug loading was determined by high performance liquid chromatography (Dionex 3000) with a UV detector at 444 nm. A Phenomenex Gemini C18 column (250 mm × 4.6 mm, 5 μ m) was used for separation at 30 °C. The mobile phase was a mixture of acetonitrile and water (9:1, v/v) with a constant flow rate at 1 mL/min and the injection volume was 20 μ L. The effect of crosslinking on the micelle stability was carried out using a method of particle sizing upon dilution [17].

2.4. *In vitro* drug release

The release of lutein from both types of micelles were carried out using the static Franz-type diffusion cells at 37 °C (n = 3) [19]. The

receiver fluid was PBS (pH 7.4, 0.15 M) with 5% SDS (w/w) and the donor phase was micelle suspension (2 mL) in PBS (pH 7.4, 0.15 M). The donor and receiver compartments were separated by a regenerated cellulose membrane (MWCO: 3500 Da). The potential membrane binding of LU was investigated by incubating LU (15 µg/mL) with the membrane (2 cm²) in the mixture of water and methanol at 37 °C; after 24 h, drug recovery was calculated (n = 3). The donor compartment was filled with RM or CM micellar solution that contained ca. 330 µg lutein. At pre-determined time points, the receiver fluid (0.5 mL) was withdrawn for drug quantification, followed by rapid supplementation of the same volume of fresh receiver fluid to maintain the total volume constant. The drug release at acidic environment utilized the citric acid-Na₂HPO₄ buffer (pH 5.0, 0.15 M) as the receiver fluid that also contained 5% (w/w) SDS to maintain the sink conditions. The release curves were presented as the cumulative amount of released drug against time.

2.5. Cytotoxicity analysis

Cervical cancer cells (HeLa cells) were obtained from the State Key Laboratory of Medicinal Chemical Biology, Nankai University. The cells were seeded in RPMI 1640 medium (Gibco, NY, USA), which containing 1% penicillin/streptomycin and 10% fetal bovine serum. HeLa cells were culturing at 37 °C with CO₂/air (5:95) humidified atmosphere. Cytotoxicity of free lutein (LU), placebo CM, drug-loaded micelles (CM/LU), placebo RM, drug-loaded micelles (RM/LU) was evaluated by the standard MTT assay. The LU dose ranged from 0 to 80 µM (n = 6). HeLa cells were seeded in 96-well plates at a density of 4 × 10³ cells/well. After 24 h incubation, five samples were added to the 96-well plates after medium removal, followed by incubating for another 48 h. The medium contained LU was removed and 100 µL of the PBS (pH 7.4, 0.01 M) was added into each well. Subsequently the cells were treated with MTT solution (100 µL, 0.5 mg/mL) for 4 h in the dark. The medium was slowly removed and 100 µL of the DMSO was added into each well to dissolve formazan. After 20 min, the absorbance of formazan is determined at 490 nm by a microplate reader (BioTek Instruments Inc., VT, USA). The percentage of viable cells and the half maximal inhibitory concentrations (IC₅₀) values were calculated accordingly.

2.6. Cell cycle analysis

Cell cycle analyses were explored by the same cell type and culture condition as cytotoxicity experiment. The cells were incubated for 24 h on 6-well plates at a seeding density of 5 × 10⁵ cells/well (n = 3). After 24 h, the medium was removed and cells were washed with 1 mL PBS (pH 7.4, 0.01 M) twice, followed by incubation for 48 h with the medium. Afterwards, the cell supernatant was removed from 6-well plate and the cells were digested with 1 mL trypsin solution for 1 min followed by adding 2 mL medium. Then the cells were washed with 1 mL ice-cold PBS (pH 7.4, 0.01 M) and suspended in 75% ethanol at 4 °C overnight. After fixation, the cell pellets were washed with ice-cold PBS in triplicate, followed by incubation with PBS solution containing 50 µg/mL PI, 100 µg/mL RNase A, and 0.2% Triton-X-100 at 4 °C for 20 min. Afterwards, the cells were analyzed by flow cytometry employing a FACSCalibur flow cytometer (Becton Dickinson, USA).

2.7. Apoptosis analysis

Detection of cell apoptosis were used the same cell type and the culture condition as cell cycle evaluation. The cells were incubated for 24 h on 6-well plates at a seeding density of 5 × 10⁵ cells/well (n = 3). After 24 h, the medium was removed and cells were washed with 1 mL PBS (pH 7.4, 0.01 M) twice, followed by sample supplementation (LU, RM/LU, CM/LU). After 48 h, the cells were centrifuged at 300 g for 5 min. The collected cells were digested with pancreatin and centrifuged at 300 g for 5 min. After that, cells were washed with 1 mL ice-

cold PBS (pH 7.4, 0.15 M) solution. The obtained cells were suspended in of binding buffer (100 µL), followed by adding Annexin V-FITC (5 µL) and PI (10 µL) staining solutions. After 15 min's incubation, the binding buffer (400 µL) was added with gentle mixing on ice. Samples were then analyzed by flow cytometry employing a FACSCalibur flow cytometer (Becton Dickinson, USA) coupled with Cell Quest Pro Software (Becton Dickinson). The cell cycle analysis was performed subsequently utilizing FlowJo software (Tree Star Inc. USA).

2.8. Statistical analysis

The data were expressed as the mean ± standard deviation (SD). A statistically significant difference was determined at a minimal level of significance of 0.05 via Student's t-test or analysis.

3. Results and discussion

3.1. Micelle preparation and characterization

Both types of polymers could successfully self-assemble into micellar nanocarriers with hydrophobic lutein being physically encapsulated. The drug loading was 3.5 ± 0.1% (w/w, RM) and 0.9 ± 0.1% (w/w, CM), respectively (Fig. 1A). The drug recovery from micelles, dialysis medium and precipitate demonstrated a LU recovery over 95% for all samples, which validated the removal of non-encapsulated drug and micelle purification. The high loading in the responsive micelles was presumed due to the potential hydrogen bonding between imidazole and lutein; the nitrogen in imidazole moiety can act as the hydrogen donor, whereas the hydroxyl group of lutein can function as the hydrogen acceptor. Such hydrogen bonding-enhanced cargo loading has also been observed in previous work [19]. The iron level in placebo RM and drug-loaded RM (RM/LU) was similar at 0.20 ± 0.01% (w/w) (Fig. 1B). This indicated that the loading process did not affect the coordination between imidazole and iron, which concurred well with previous report [17]. However, the presence of lutein slightly increased the hydrodynamic size of micelles irrespective of the micelle type and medium acidity (p < 0.05) (Fig. 1C and D). Polymeric micelles often display a hydrophobic core-hydrophilic shell structure with the hydrophobic cargos locating in the core. Upon drug loading, the drug would occupy some space to enable core expansion, leading to an enlarged micelle [27], which was the case in the current study. Regarding the responsive micelles, the hydrodynamic diameters increased clearly with decreasing pH. As the micelle self-assembly is

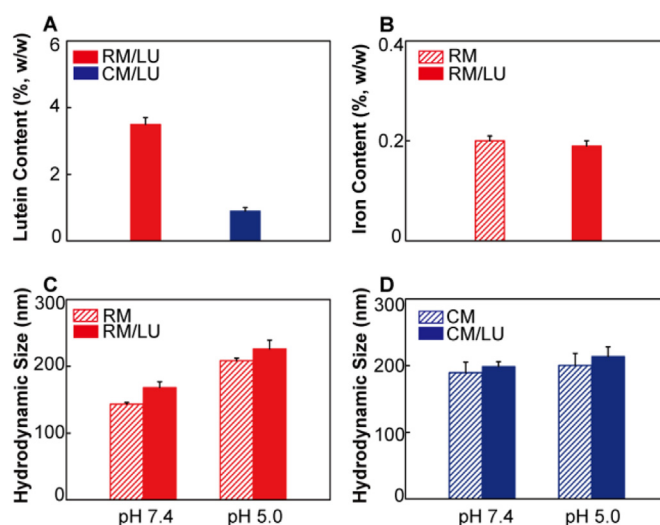


Fig. 1. Pharmaceutical assessment of lutein (LU)-loaded crosslinked responsive micelles (RM) and control micelles (CM) (n = 3). (A) Drug loading; (B) Iron loading; (C–D) Hydrodynamic size.

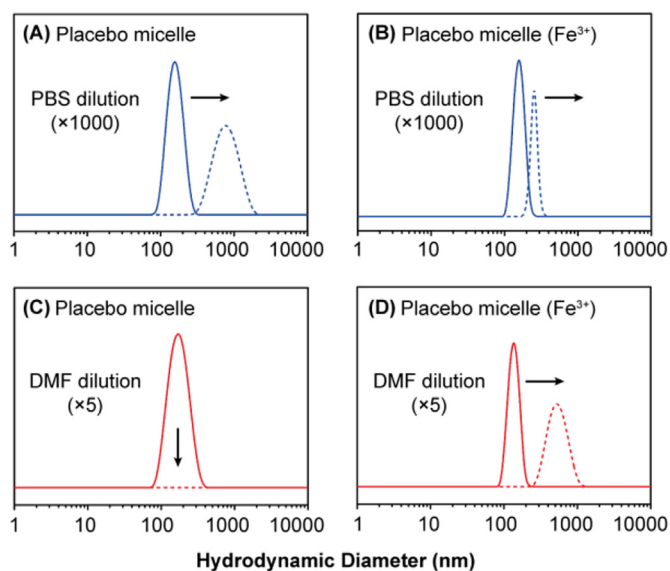


Fig. 2. Stability assessment of placebo responsive micelles (RM) via dilution with PBS or DMF. The hydrodynamic size of micelles was used as the indicator. The micelle concentration was set at 1 mg/mL prior to dilution for all samples; the ratio of dilution in PBS (A, B) and DMF (C, D) was 1000 and 5 times, respectively. The symbol (Fe^{3+}) represents imidazole- Fe^{3+} coordinated micelle core cross-linking.

precisely controlled by the interplay of copolymer amphiphilicity, architecture and conformation, crystallinity of hydrophobic segment, hydrogen bonding, host-guest interaction, and stereo-complexation [28], the increased degree of ionization of imidazole moiety at low pH would impair the coordination network and shift the amphiphilicity of the copolymer towards the direction of hydrophilicity, resulting in micelle expansion. The crosslinked CM micelles via imidazole-iron coordination displayed enhanced stability, which was demonstrated by the particle size comparison against un-crosslinked micelles upon dilution (Fig. 2). This trend was consistent with previous report that employed catechol-iron crosslinked micelles [17].

3.2. *In vitro* drug release

The rapid cargo release from nanocarriers is critical for an efficient delivery system [15,20]. A poor drug release may result in a low intracellular drug level that is below the minimum effective concentration, leading to no efficacy. In addition, the poor drug release can also delay the onset of pharmacological action of the active pharmaceutical ingredients (API), which is unacceptable for those symptoms or diseases that need rapid medicine treatment. In the current study, LU showed no binding with the membrane, as evidenced by good drug recovery (> 98%) post 24h incubation with the membrane. The cumulative LU release from the responsive micelles (RM) was significantly higher under the condition of pH 5.0 compared to that at pH 7.4 (Fig. 3A). The release profile of LU from non-crosslinked RM was similar to that of crosslinked RM; at a fixed pH, the extent of drug release was higher compared to that with iron crosslinking (Fig. 3B). However, the drug release profiles from non-responsive control micelles (CM) at pH 7.4 and pH 5.0 are almost identical (Fig. 3C). Since all types of micelles encapsulated the same drug (LU), the dose in the donor compartment was kept the same. Such discrepancy regarding LU release was a consequence of the loss of imidazole-iron coordination bonding at low pH and hence the disassembly and expansion of responsive micelles. The ionization of imidazole moiety in the acidic conditions further increased the hydrophilicity of the mPEG-PAsp-IM copolymer, which would have a positive influence in micelle disassembly and accelerated drug release. Upon micelle expansion, the water can easily penetrate into the core of micelles where the drug locates, followed by facilitated

drug dissolution, and diffusion out of the micelle into the medium [14]. Usually the stability of polymeric micelles is controlled by multiple factors, including the type, amphiphilicity and architecture of polymers, the presence of crosslinking, the nature of dispersion medium. For the CM in the current work, pH was a key regulator as the extent of crosslinking was directly linked to the medium acidity. A lower pH would damage the crosslinking and induce micelle disassembly, which was evidenced by the accelerated drug release from CM micelles at pH 5.0 (Fig. 3A and B).

3.3. Cytotoxicity

The MTT test revealed that the IC_{50} of free LU in HeLa cells was $33.1 \pm 3.8 \mu\text{M}$; the corresponding IC_{50} of drug-loaded micelles was $58.4 \pm 9.6 \mu\text{M}$ (RM/LU) (Fig. 4A). In contrast, the control micelles (CM/LU) displayed a much lower cytotoxicity (Fig. 4A). We first ruled out the effect of polymers on cell viability and both types of placebo micelles are almost non-toxic up to a carrier concentration of 40 $\mu\text{g}/\text{mL}$ (Fig. 4B). The higher cytotoxicity of free lutein in comparison to that of responsive micelles (RM/LU) was because the micelles had to experience a drug release process before exerting the toxic effect, while the free lutein formulation didn't have such step. Likewise, the IC_{50} variance between responsive micelles and control micelles was again the consequence of the different rate and extent to which the drug was released from the nanocarriers (Fig. 3). Therefore, it was the pH-responsive characteristic of the RM/LU micelles that caused the enhanced cytotoxicity.

3.4. Cell cycle analysis

Despite the increasing attention to the anti-cancer effect of lutein, the exact mechanism(s) by which this natural compound exerts the cytotoxic action has not been clarified based on the literature available. We first examined the capability of lutein and lutein-loaded micelles in regulating cell cycle. The results showed that both free lutein and lutein-loaded two types of micelles (RM and CM) induced cell cycle arrest in G_2/M phase compared to the control cells without any formulation treatment (Fig. 5). Due to the slow drug release from non-responsive CM nanosystem, the degree of G_2/M arrest is lower than that of free lutein and RM micelles. A previous investigation also reported that lutein improved drug-induced cell cycle arrest in prostate cancer (PC-3) cells [29]. Nevertheless, the lutein-induced G_2/M phase cell cycle arrest observed in the current study was less evident, indicating that lutein was not a potent cell cycle regulator. Hence, the lutein-initiated cytotoxicity might be only partly contributed by the cell cycle arrest in G_2/M phase.

3.5. Apoptosis analysis

We further performed the apoptosis experiments to demonstrate the influence of drug release on the anti-cancer effect of lutein at the cellular level. The free lutein (LU), non-responsive micelles (CM/LU) and pH-responsive micelles (RM/LU) all exhibited significant apoptotic consequence compared to the control without any sample challenge (Fig. 6). The degree of apoptosis ranked as follows: LU > RM/LU > CM/LU. The control sample didn't show any apoptotic signal. As the free LU didn't have the release barrier, the highest apoptosis extent (ca. 83%) was observed. Regarding both nanocarriers, the pH-cleavable micelles could enable a rapid lutein release due to the pH-triggered de-crosslinking and micelle disassembly. Hence a significantly higher degree of apoptosis was obtained compared to that of non-responsive micelles (74% vs. 50%). The apoptosis data agreed well with the *in vitro* drug release behavior.

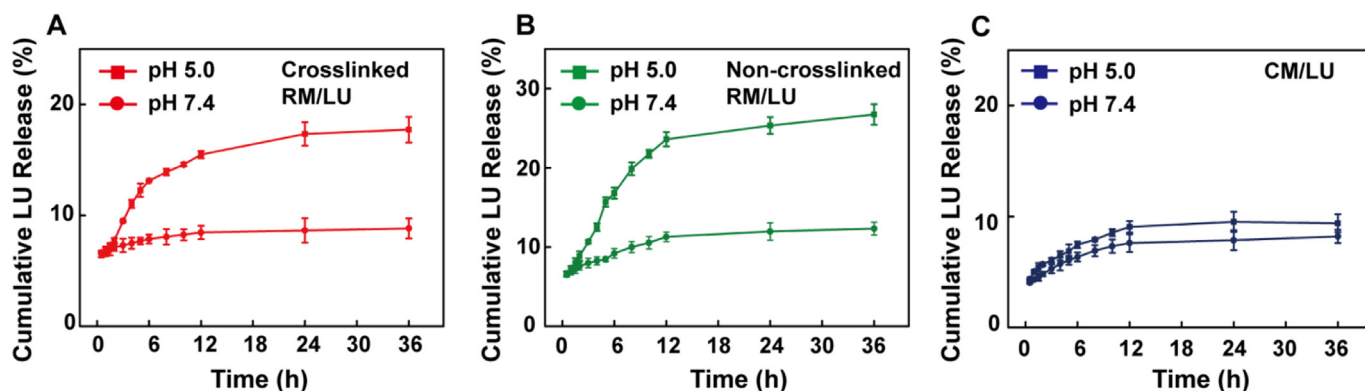


Fig. 3. Cumulative release of lutein from (A) pH-responsive crosslinked micelles (RM/LU), (B) pH-responsive non-crosslinked micelles (RM/LU), and (C) non-responsive control micelles (CM/LU) under two different pH conditions.

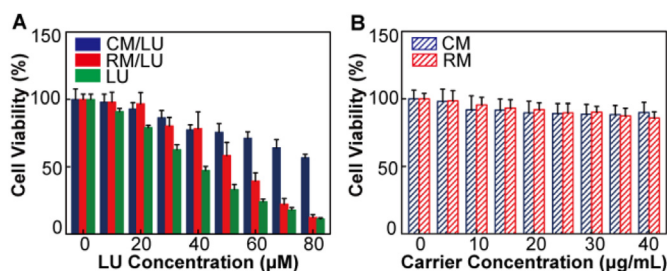


Fig. 4. Viability of HeLa cells in response to five different formulations (n = 4). (A) Free lutein (LU), drug-loaded micelles (CM/LU and RM/LU); (B) Placebo micelles (CM and RM).

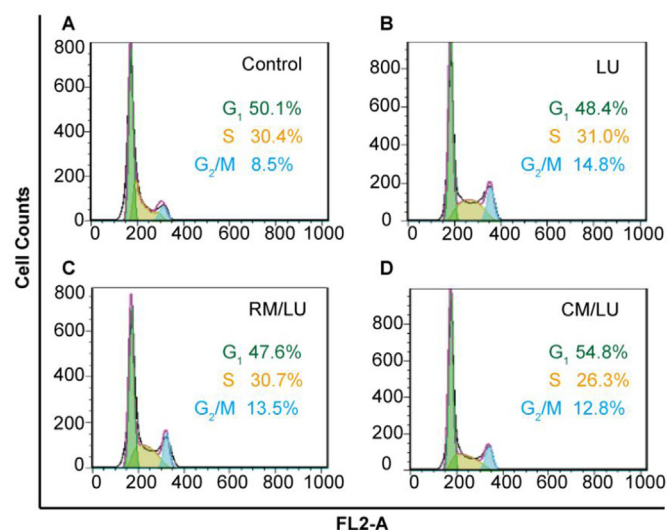


Fig. 5. Cell cycle analysis of HeLa cells treated with free lutein (LU) and lutein-loaded micelles (CM/LU and RM/LU).

4. Conclusion

In summary, we report a pH-responsive polymeric micellar nano-carrier to realize acid-triggered delivery of lutein for anti-cancer therapy. The imidazole moiety in the polymer is the key for on-demand lutein release because the imidazole can be ionized and hence shift the hydrophobic segments of the polymer towards hydrophilic counterpart, resulting in micelle disassembly and drug release. The rapid lutein release indeed had a positive effect on the cytotoxicity due to the elevated intracellular concentration of free drug. Further cell cycle and apoptosis analysis concurred well with the cell viability assay. The current work provides a facile nanoplatform for improved aqueous solubility and on-

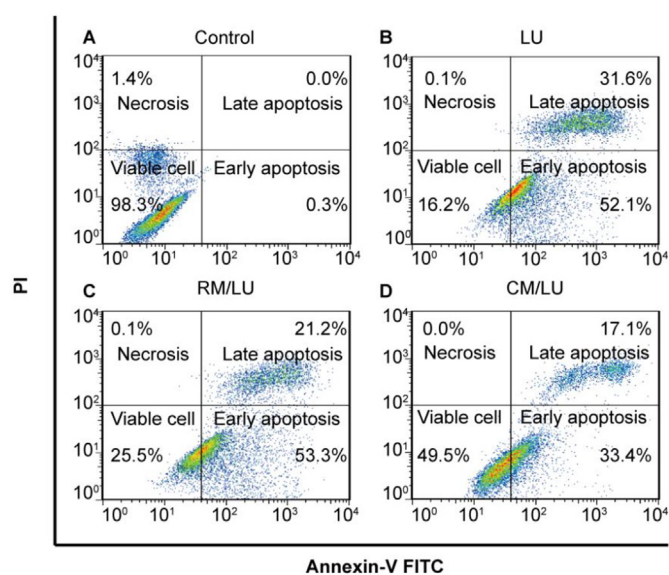


Fig. 6. Apoptotic analysis of HeLa cells treated by four different formulations (A) control; (B) free lutein (LU); (C) pH-responsive lutein-loaded micelles (RM/LU); (D) non-responsive lutein-loaded control micelles (CM/LU).

demand delivery of lutein, which can be easily extended to other types of carotenoids.

Conflicts of interest

The authors declare no conflicts of interest.

References

- [1] R. Tsao, M. Wang, Z. Deng, Lutein: separation, antioxidant activity, and potential health benefits, antioxidant measurement and applications, in: F. Shahidi, C.T. Ho (Eds.), *Antioxidant Measurement and Applications*, American Chemical Society, Washington, 2007, pp. 352–372.
- [2] N.K. Scripsema, D.N. Hu, R.B. Rosen, Lutein, zeaxanthin, and meso-zeaxanthin in the clinical management of eye disease, *J. Ophthalmol.* 2015 (2015) 865179.
- [3] A. Milani, M. Basirnejad, S. Shahbazi, A. Bolhassani, Carotenoids: biochemistry, pharmacology and treatment, *Br. J. Pharmacol.* 174 (2017) 1290–1324.
- [4] E.R. Sindhu, R. Kuttan, Carotenoid lutein protects the kidney against cisplatin-induced acute renal failure, *J. Environ. Pathol. Toxicol. Oncol.* 32 (2013) 21–28.
- [5] Y. Jiao, X. Zheng, Y. Chang, D. Li, X. Sun, X. Liu, Zein-derived peptides as nano-carriers to increase the water solubility and stability of lutein, *Food Funct.* 9 (2018) 117–123.
- [6] K. Mitri, R. Shegokar, S. Gohla, C. Anselmi, R.H. Muller, Lipid nanocarriers for dermal delivery of lutein: preparation, characterization, stability and performance, *Int. J. Pharm.* 414 (2011) 267–275.
- [7] K. Mitri, R. Shegokar, S. Gohla, C. Anselmi, R.H. Muller, Lutein nanocrystals as antioxidant formulation for oral and dermal delivery, *Int. J. Pharm.* 420 (2011) 141–146.

- [8] C.H. Liu, H.C. Chiu, W.C. Wu, S.L. Sahoo, C.Y. Hsu, Novel lutein loaded lipid nanoparticles on porcine corneal distribution, *J. Ophthalmol.* 2014 (2014) 304694.
- [9] R. Arunkumar, K.V.H. Prashanth, Y. Manabe, T. Hirata, T. Sugawara, S.M. Dharmesh, V. Baskaran, Biodegradable poly (lactic-co-glycolic acid)-poly-ethylene glycol nanocapsules: an efficient Carrier for improved solubility, bioavailability, and anticancer property of lutein, *J. Pharmacol. Sci.* 104 (2015) 2085–2093.
- [10] A. Ranganathan, R. Hindupur, B. Vallikannan, Biocompatible lutein-polymer-lipid nanocapsules: acute and subacute toxicity and bioavailability in mice, *Mater. Sci. Eng. C Mater. Biol. Appl.* 69 (2016) 1318–1327.
- [11] E. Blanco, H. Shen, M. Ferrari, Principles of nanoparticle design for overcoming biological barriers to drug delivery, *Nat. Biotechnol.* 33 (2015) 941–951.
- [12] Y. Zhao, M.B. Brown, S.A. Jones, Pharmaceutical foams: are they the answer to the dilemma of topical nanoparticles? *Nanomedicine* 6 (2010) 227–236.
- [13] C. Guo, Y. Zhang, M. Sun, Z. Wang, A. Fan, Y. Zhao, Modulating topical drug delivery via skin pre-treatment with low-generation poly(amidoamine) dendrimers, *J. Drug Deliv. Sci. Technol.* 24 (2014) 555–557.
- [14] Z. Wang, C. Chen, Q. Zhang, M. Gao, J. Zhang, D. Kong, Y. Zhao, Tuning the architecture of polymeric conjugate to mediate intracellular delivery of pleiotropic curcumin, *Eur. J. Pharm. Biopharm.* 90 (2015) 53–62.
- [15] S. Mura, J. Nicolas, P. Couvreur, Stimuli-responsive nanocarriers for drug delivery, *Nat. Mater.* 12 (2013) 991–1003.
- [16] N.A. Stocke, S.M. Arnold, J.Z. Hilt, Responsive hydrogel nanoparticles for pulmonary delivery, *J. Drug Deliv. Sci. Technol.* 29 (2015) 143–151.
- [17] K. Xin, M. Li, D. Lu, X. Meng, J. Deng, D. Kong, D. Ding, Z. Wang, Y. Zhao, Bioinspired coordination micelles integrating high stability, triggered cargo release, and magnetic resonance imaging, *ACS Appl. Mater. Interfaces* 9 (2017) 80–91.
- [18] Y. Cao, M. Gao, C. Chen, A. Fan, J. Zhang, D. Kong, Z. Wang, D. Peer, Y. Zhao, Triggered-release polymeric conjugate micelles for on-demand intracellular drug delivery, *Nanotechnology* 26 (2015) 115101.
- [19] X. Li, M. Gao, K. Xin, L. Zhang, D. Ding, D. Kong, Z. Wang, Y. Shi, F. Kiessling, T. Lammers, J. Cheng, Y. Zhao, Singlet oxygen-responsive micelles for enhanced photodynamic therapy, *J. Contr. Release* 260 (2017) 12–21.
- [20] V.P. Torchilin, Multifunctional, stimuli-sensitive nanoparticulate systems for drug delivery, *Nat. Rev. Drug Discov.* 13 (2014) 813–827.
- [21] H. Li, M. Li, C. Chen, A. Fan, D. Kong, Z. Wang, Y. Zhao, On-demand combinational delivery of curcumin and doxorubicin via a pH-labile micellar nanocarrier, *Int. J. Pharm.* 495 (2015) 572–578.
- [22] M. Li, M. Gao, Y. Fu, C. Chen, X. Meng, A. Fan, D. Kong, Z. Wang, Y. Zhao, Acetal-linked polymeric prodrug micelles for enhanced curcumin delivery, *Colloids Surfaces B Biointerfaces* 140 (2016) 11–18.
- [23] E.B. Anderson, T.E. Long, Imidazole- and imidazolium-containing polymers for biology and material science applications, *Polymer* 51 (2010) 2447–2454.
- [24] J.E. Bauman, J.C. Wang, Imidazole complexes of nickel(II), copper(II), zinc(II), and silver(I), *Inorg. Chem.* 3 (1964) 368–373.
- [25] P. Gao, L. Zheng, L. Liang, X. Yang, Y. Li, C. Huang, A new type of pH-responsive coordination polymer sphere as a vehicle for targeted anticancer drug delivery and sustained release, *J. Mater. Chem. B* 1 (2013) 3202–3208.
- [26] Y. He, L. Xing, P. Cui, J. Zhang, Y. Zhu, J. Qiao, J. Lyu, M. Zhang, C. Luo, Y. Zhou, N. Lu, H. Jiang, Transferrin-inspired vehicles based on pH-responsive coordination bond to combat multidrug-resistant breast cancer, *Biomaterials* 113 (2017) 266–278.
- [27] V.P. Torchilin, Micellar nanocarriers: pharmaceutical perspectives, *Pharm. Res.* 24 (2007) 1–16.
- [28] X. Dong, X. Guo, G. Liu, A. Fan, Z. Wang, Y. Zhao, When self-assembly meets topology: an enhanced micelle stability, *Chem. Commun.* 53 (2017) 3822–3825.
- [29] M.M. Rafi, S. Kanakasabai, S.V. Gokarn, E.G. Krueger, J.J. Bright, Dietary lutein modulates growth and survival genes in prostate cancer cells, *J. Med. Food* 18 (2015) 173–181.